AAS 03-518

ESTIMATION OF INSTANTANEOUS MANEUVERS USING A FIXED INTERVAL SMOOTHER

James Woodburn=

John Carrico♀

James R. Wright☼

An alternative to the typical means of maneuver reconstruction and calibration is presented which uses the orbit determination process to directly provide an estimate of short duration orbital maneuvers. The proposed method uses a sequential filter and fixed interval smoother to estimate the satellite state forward and backward across the time of the maneuver. The resulting maneuver estimate, which is derived directly from the output of the smoother, is supplemented by the existence of an associated covariance. Examples of this process using both real and simulated tracking data are presented in conjunction with a comparison to standard reconstruction and calibration methods using least squares.

INTRODUCTION

Orbital maneuvers are part of normal operations for many satellites. Maneuvers are performed for a variety of reasons including the establishment and maintenance of the operational orbit. The operational execution of maneuvers usually contains both a maneuver planning phase and post-maneuver analysis to calibrate the maneuver. The maneuver planning process typically includes a verification that all mission constraints are being met prior to, during and after the maneuver in addition to design of the desired maneuver. Post-maneuver analysis strives to determine the actual maneuver resulting from the thrusting by using orbit determination results from tracking prior to and after the maneuver. This process, sometimes referred to as maneuver reconstruction and calibration, is often done by applying the maneuver design tools to determine the maneuver required to link the pre-maneuver orbit estimate to the post maneuver orbit estimate. The reconstructed maneuver is then analyzed to yield calibration information such as the efficiency of the engine and the presence of errors in the thrust direction.

= Chief Orbital Scientist, Analytical Graphics, Inc., Senior Member AIAA, Member AAS
♀ Senior Astrodynamics Specialist, Analytical Graphics, Inc., Member, AAS
☼ Senior Engineer, Analytical Graphics, Inc.

There are two main reasons to calibrate a maneuver after it has been executed by the spacecraft. The first is to assess the success of the maneuver and to determine if any corrective action must be taken, either a fine 'vernier' correction or possibly a quick major energy correction in the case of a drastically under-performing engine. The second reason for calibrating is to establish a trend in the overall propulsion system performance. Usually after a few maneuvers it is possible to calibrate the system and to use the resulting calibration factor when planning subsequent maneuvers. For instance, when planning a maneuver using a propulsion system calibrated at two percent 'cold' (underperformance), the analyst may purposely increase the duration of the next maneuver by two percent to eliminate the need for additional maneuvers.

Many orbit maintenance maneuvers, such as those used for groundtrack control or drag make-up, are small in magnitude and are typically executed over a very short duration relative to the orbital period of the satellite. In such cases, the maneuvers may be modeled as instantaneous events to a high degree of accuracy. Maneuvers of larger magnitude can also be accurately modeled as being instantaneous if a high thrust engine is used and the burn duration remains small relative to the orbital period. The analysis of these nearly instantaneous maneuvers is the focus of this study.

CONVENTIONAL MANEUVER ESTIMATION AND CALIBRATION

Most algorithms for maneuver calibration are based on the use of estimates of the orbit produced by least squares orbit determination processes. The basic idea is to determine the maneuver that connects a pre-maneuver orbit estimate to a post-maneuver orbit estimate. A fairly simple method commonly used to determine the effectiveness of a maneuver involves the analyst determining the point of closest approach of the pre-maneuver orbit estimate to the post-maneuver orbit estimate and taking the difference of the velocity components to be the observed instantaneous maneuver, DV_O. An efficiency factor can be calculated by comparing this to the planned (desired) maneuver, DV_P:

$$e = 1 + \frac{\left|\Delta \mathbf{V}_O - \Delta \mathbf{V}_P\right|}{\left|\Delta \mathbf{V}_P\right|}$$

This method is more accurate when the duration of the maneuver is small so that the approximation at the point of closest approach is small. A comparison of the vector difference between the planned and observed maneuvers may also give an indication of any error in the direction of the maneuver. We note that this method does not account for the discontinuity in position at the time of closest approach nor does it provide a measure of confidence in the estimated maneuver. Further, the time of closest approach may differ from the known centroid of the maneuver.

Another common method to calibrate a maneuver is to examine the effect on an orbital element expected to change as a result of the maneuver. For example, many maneuvers are designed to only affect the semi-major axis. The pre-maneuver semi-major axis, a_i, can be calculated from the pre-maneuver state. Likewise, a post-maneuver semi-

major axis, a_f, can be calculated from the planned post-maneuver trajectory. An efficiency can be calculated as:

$$e = \frac{a_O - a_i}{a_f - a_i},$$

where a_0 is the semi-major axis calculated from the observed post maneuver trajectory. This technique is applicable to longer duration burns, but does not yield any insight into errors in thrust direction.

Variations on these techniques are also used. Sometimes the efficiency is put back into the maneuver planning software and the maneuver is reconstructed to compare with the observed parameter. This process is then repeated with the efficiency factor differentially corrected until the difference between the observed and predicted parameter is considered small.

A more robust technique employs multi-dimensional differential corrections with least squares to simultaneously estimate the efficiency factor and direction errors[1]. In this method, most conveniently performed with software, the orbit estimate at the time of maneuver ignition taken from the pre-maneuver orbit determination result is used as the starting point. The software then reconstructs the maneuver to calculate a post-maneuver orbit state. This post maneuver reconstructed orbit state, $\vec{X}_R$, can be compared with the post-maneuver orbit estimate, $\vec{X}_O$, to determine how well the maneuver was modeled. By numerically perturbing some of the maneuver modeling independent parameters a sensitivity matrix, $\bar{S}$, can be constructed, with each term representing the change in one component of $\vec{X}_O$ as a function of one independent parameter. $\vec{X}_O$ is typically represented as the six Keplerian elements. The independent parameters for finite burns are usually a thrust efficiency factor and two pointing controls such as pitch and yaw. For impulsive burns, the instantaneous change in velocity, $\Delta\vec{V}$, vector can be used. In both cases, the size of $\bar{S}$ is 6 rows by 3 columns. A least squares technique is then used to compute a linear estimate of the correction to the independent parameters. Adding the corrections to the parameters used during planning, the maneuver is again reconstructed, and the process repeated until the corrections to the parameters are considered small. In this procedure, the position discontinuity is removed, but there is still no information available regarding a confidence level in the result.

AN ALTERNATIVE APPROACH

In this paper we present an alternative to the typical maneuver reconstruction and calibration procedure. This alternative method uses the orbit determination system directly to provide an estimate of an instantaneous maneuver. The orbit determination method consists of a sequential filter used to move forward across the maneuver and a fixed interval smoother to move backwards across the maneuver. The sequential filter serves to process all

of the tracking data prior to the maneuver to provide an optimal pre-maneuver state estimate and covariance. The sequential filter then continues across the maneuver, adding the uncertainty in the maneuver to the velocity sub-matrix of the covariance. Tracking data is processed after the time of the maneuver until the uncertainty in the state estimate returns to a normal non-maneuver condition. At that time, the filter state and covariance are used to initialize the fixed interval smoother and the smoothing process is run backwards until a time prior to the maneuver. The smoother serves to map information provided by the post-maneuver tracking data backwards and provides a smoothed estimate of the post-maneuver state. The smoothing process continues across the time of the maneuver to yield a smoothed estimate of the pre-maneuver state. The difference between the pre-maneuver and post-maneuver smoothed states may now be extracted as the estimate of the maneuver. The pre-maneuver and post-maneuver smoothed covariance matrices are used to compute the uncertainty associated with the estimate of the maneuver. It is noteworthy that no additional states are added to the estimation process and that this solution can be done in the process of normal operations without the need for additional tasks being performed by orbit analysts.

NOTATION

The following notational conventions are used:

Variables

t	time
X	true state
$\hat{X}$	Filter estimate of state
$\tilde{X}$	Smooth estimate of state
$d\hat{X}$	Error in filter estimate of state
$d\tilde{X}$	Error in smooth estimate of state
$\hat{P}$	Filter estimate of state error covariance
$\tilde{P}$	Smooth estimate of state error covariance
$P^{\int\int}$	Filter process noise covariance
f	Linear state error transition matrix
J	Non-linear state transition function

$\Delta X_{\Delta V}$ Nominal state change at instantaneous maneuver

$P_{\Delta V}^{\iint}$ Error covariance on nominal maneuver

$\Delta \tilde{\tilde{X}}_{\Delta V}$ Smooth estimate of instantaneous maneuver

$\tilde{\tilde{P}}_{\Delta V}$ Smooth estimate of instantaneous maneuver error covariance

$d\tilde{\tilde{X}}_{\Delta V}$ Error in smooth estimate of instantaneous maneuver

Subscripts

t_k	kth entry of a set of discrete times $(t_0, t_1, t_2, ...)$
k	at time t_k
$k+1 \mid k$	Estimate at t_{k+1} incorporating measurements up to t_k
$k+1, k$	Transition from t_k to t_{k+1}
c	at the time of the maneuver centroid

FORMULATION

Since the estimate of the instantaneous maneuver is extracted from the smoothed state estimate history and the smoother operates on data produced by the filter, the maneuver must be modeled in the filter processing. The filter process consists of series of time updates and measurement updates. The time update procedure serves to move the filter state estimate and state error covariance forward in time from one measurement to the next. The measurement update serves to provide a new estimate of the state and state error covariance at the time of a measurement based on the information contained in the measurement. The instantaneous maneuver is accounted for in the filter via incorporation in the time update algorithm. The time update is formulated as:

$$\hat{X}_{k+1|k} = J(\hat{X}_{k|k}, t_k, t_{k+1}), \tag{1}$$

$$P_{k+1|k} = f_{k+1,k}\ P_{k|k}\ f_{k+1,k}^{T} + P_{k+1|k}^{\iint}, \tag{2}$$

where $J(\hat{X}_{k|k}, t_k, t_{k+1})$ represents the nonlinear transition of the filter state estimate, $\hat{X}$, from time t_k to time t_{k+1}. We define a maneuver centered on time t_c and having a duration of e such that

$$\left(t_k = t_c - \frac{e}{2}\right) < t_c < \left(t_c + \frac{e}{2} = t_{k+1}\right).$$

For the case of an instantaneous maneuver where $e \to 0$,

$$t_k = \lim_{e\to 0}\left(t_c - \frac{e}{2}\right),$$

$$t_{k+1} = \lim_{e\to 0}\left(t_c + \frac{e}{2}\right),$$

the non-linear state transition simply consists of adding the instantaneous change in velocity to the velocity components in the state. The state error transition matrix, $f_{k+1,k}$, is the identity matrix and the process noise covariance is the covariance associated with the maneuver. The time update formulation across an instantaneous maneuver in the filter may therefore be written as,

$$\hat{X}_{k+1|k} = \hat{X}_{k|k} + \Delta X_{\Delta V}, \tag{3}$$

$$P_{k+1|k} = P_{k|k} + P_{\Delta V}^{\iint}. \tag{4}$$

As the filter processes information in the forward direction, information is saved to support the smoothing process. The inputs to the smoother resulting from a filter time update consist of the updated state, the updated covariance and the process noise covariance.

The smoothing process starts with the initial smoothed state estimate and state error covariance equal to the last estimates available from the filter. If we stop the filter at the time of the last measurement, t_L, then the smoother is initialized as,

$$\tilde{X}_{L|L} = \hat{X}_{L|L}, \tag{5}$$

$$\tilde{P}_{L|L} = \hat{P}_{L|L}. \tag{6}$$

The smoothing process then proceeds in the reverse time direction combining the current smoothed estimate and state error covariance with the filtered estimates according to[2,3],

$$\tilde{X}_{k|L} = \hat{X}_{k|k} + \hat{P}_{k|k}\left[\hat{P}_{k|k} + f_{k+1,k}^{-1}\, P_{k+1|k}^{\iint}\left(f_{k+1,k}^{-1}\right)^T\right]^{-1}\left[J\left(\tilde{X}_{k+1|L}, t_{k+1}, t_k\right) - \hat{X}_{k|k}\right], \tag{7}$$

$$\tilde{P}_{k|L} = \hat{P}_{k|k} + A_{k,k+1}\left[\tilde{P}_{k+1|L} - \hat{P}_{k+1|k}\right]A_{k,k+1}^T, \tag{8}$$

where,

$$A_{k,k+1} = \hat{P}_{k|k}\, f^{T}_{k+1,k} \hat{P}^{-1}_{k+1|k}. \tag{9}$$

Eqs (7-8) present a modification of the smoother implementation given in Meditch[1] and Rauch[2] to use a full non-linear state transition to move the state estimate backwards in time. In the case where the smoother traverses an instantaneous maneuver, the non-linear state transition simplifies to

$$J\left(\tilde{\tilde{X}}_{k+1|L}, t_{k+1}, t_k\right) = \tilde{\tilde{X}}_{k+1|L} - \Delta X_{\Delta V}. \tag{10}$$

Recalling that the state error transition matrix, $f_{k+1,k}$, becomes the identity matrix, Eqs. (7-8) may be simplified to

$$\tilde{\tilde{X}}_{k|L} = \hat{X}_{k|k} + \hat{P}_{k|k}\left[\hat{P}_{k|k} + P^{\iint}_{\Delta V}\right]^{-1}\left[\left(\tilde{\tilde{X}}_{k+1|L} - \Delta X_{\Delta V}\right) - \hat{X}_{k|k}\right], \tag{11}$$

$$\tilde{\tilde{P}}_{k|L} = \hat{P}_{k|k} + A_{k,k+1}\left[\tilde{\tilde{P}}_{k+1|L} - \hat{P}_{k+1|k}\right]A^{T}_{k,k+1}, \tag{12}$$

where,

$$A_{k,k+1} = \hat{P}_{k|k}\, \hat{P}^{-1}_{k+1|k}.$$

We recall that the above simplifications are possible due to transition across an instantaneous maneuver, $t_k = t_{k+1}$. The smoothed estimate of the instantaneous maneuver is then given by differencing the smoothed pre-maneuver and post-maneuver states,

$$\tilde{\tilde{X}}_{\Delta V} = \tilde{\tilde{X}}_{k+1|L} - \tilde{\tilde{X}}_{k|L}. \tag{13}$$

The error covariance of the maneuver estimate is formally expressed as,

$$\tilde{\tilde{P}}_{\Delta V} = E\left[\left(d\tilde{\tilde{X}}_{k+1|L} - d\tilde{\tilde{X}}_{k|L}\right)\left(d\tilde{\tilde{X}}_{k+1|L} - d\tilde{\tilde{X}}_{k|L}\right)^{T}\right], \tag{14}$$

which can be expanded to the form

$$\tilde{\tilde{P}}_{\Delta V} = \tilde{\tilde{P}}_{k|L} + \tilde{\tilde{P}}_{k+1|L} - E\left[d\tilde{\tilde{X}}_{k|L} d\tilde{\tilde{X}}^{T}_{k+1|L}\right] - E\left[d\tilde{\tilde{X}}_{k+1|L} d\tilde{\tilde{X}}^{T}_{k|L}\right], \tag{15}$$

Eq. (15) implies that the covariance of the maneuver estimate would simply be equal to the sum of the pre-maneuver and post-maneuver covariance matrices if the pre-maneuver and post maneuver states were not correlated. Note that last two terms of Eq. (15) are not symmetric, but the sum of these terms is symmetric. The error form of Eq. (11) gives the relationship between pre-maneuver smoothed errors and post-maneuver smoothed errors,

$$d\tilde{\tilde{X}}_{k|L} = d\hat{X}_{k|k} + \hat{P}_{k|k}\left[\hat{P}_{k|k} + P^{\iint}_{\Delta V}\right]^{-1}\left[d\tilde{\tilde{X}}_{k+1|L} - d\hat{X}_{k|k}\right]. \tag{16}$$

Both sides of Eq. (16) are post multiplied by $d\tilde{\tilde{X}}^{T}_{k+1|L}$ to yield,

$$d\tilde{\tilde{X}}_{k|L} d\tilde{\tilde{X}}^{T}_{k+1|L} = d\hat{X}_{k|k} d\tilde{\tilde{X}}^{T}_{k+1|L} + \hat{P}_{k|k}\left[\hat{P}_{k|k} + P^{\iint}_{\Delta V}\right]^{-1}\left[d\tilde{\tilde{X}}_{k+1|L} - d\hat{X}_{k|k}\right] d\tilde{\tilde{X}}^{T}_{k+1|L}. \tag{17}$$

Apply the expectation operator to both sides of Eq. (17) and rearrange terms to give

$$E\left[d\tilde{X}_{k|L}d\tilde{X}^{T}_{k+1|L}\right]= A_{k,k+1}\tilde{P}_{k+1|L}+\left[I-A_{k,k+1}\right]E\left[d\hat{X}_{k|k}d\tilde{X}^{T}_{k+1|L}\right], \quad (18)$$

where

$$A_{k,k+1}=\hat{P}_{k|k}\,\hat{P}^{-1}_{k+1|k}=\hat{P}_{k|k}\left[\hat{P}_{k|k}+P^{\iint}_{\Delta V}\right]^{-1}.$$

Since the first term on the right hand side of Eq. (18) is symmetric, substituting this result into Eq. (15) to yields,

$$\tilde{P}_{\Delta V}=\tilde{P}_{k|L}+\tilde{P}_{k+1|L}-2A_{k,k+1}\tilde{P}_{k+1|L}-\left[I-A_{k,k+1}\right]\left\{E\left[d\hat{X}_{k|k}d\tilde{X}^{T}_{k+1|L}\right]+E\left[d\tilde{X}_{k+1|L}d\hat{X}^{T}_{k|k}\right]\right\}. \quad (19)$$

Computation of the last term requires a model of the cross covariance between the pre-maneuver estimate from the filter and the post-maneuver estimate from the smoother. However, the significance of this cross covariance should diminish as the number of processed measurements after the time of the maneuver increases and as the time span of measurements after the time of the maneuver increases. The cross covariance is multiplied by a positive definite matrix, $\left[I-A_{k,k+1}\right]$, which ranges from the identity matrix when the uncertainty in the maneuver is large to a zero matrix when knowledge of the maneuver is perfect. In lieu of constructing a model for the computation of the cross covariance, we assume that the contribution of the cross covariance on the complete maneuver error covariance will be small given that enough measurements are processed after the time of the maneuver and that the orbit is observable based on those measurements. Since the cross covariance term would serve to reduce the size of the maneuver error covariance, the maneuver error covariance computed by ignoring the cross covariance should be conservative. The following is therefore the proposed computation for the maneuver estimate covariance:

$$\tilde{P}_{\Delta V}\cong\tilde{P}_{k|L}+\tilde{P}_{k+1|L}-2A_{k,k+1}\tilde{P}_{k+1|L}. \quad (20)$$

Special Cases

Some insight into the expression given in Eq. (19) can be gained by examining the meaning of the last two terms on the right hand side. $A_{k,k+1}$ approaches the unit matrix as the uncertainty in the maneuver approaches zero, but $A_{k,k+1}$ approaches zero as the uncertainty in the maneuver becomes large. For the case where the *apriori* uncertainty in the maneuver is zero, Eq. (19) simplifies to,

$$\tilde{P}_{\Delta V}=\tilde{P}_{k|L}-\tilde{P}_{k+1|L}. \quad (21)$$

If we substitute the identity matrix for $A_{k,k+1}$ in Eq. (8), we see that

$$\tilde{P}_{k|L}=\hat{P}_{k|k}+\tilde{P}_{k+1|L}-\hat{P}_{k+1|k}, \quad (22)$$

for which Eq. (21) is simplified to the expected result,

$$\tilde{P}_{\Delta V}=0. \quad (23)$$

If, on the other hand, the uncertainty in the maneuver is large, then Eq. (19) simplifies to,

$$\tilde{P}_{\Delta V} = \tilde{P}_{k|L} + \tilde{P}_{k+1|L} - \left\{ E\left[d\hat{X}_{k|k} d\tilde{X}^{T}_{k+1|L} \right] + E\left[d\tilde{X}_{k+1|L} d\hat{X}^{T}_{k|k} \right] \right\}. \quad (24)$$

Assuming that a sufficient number of measurements are processed after the time of the maneuver, the correlation between the pre-maneuver filter errors and the post-maneuver smoother errors becomes small and Eq. (24) simplifies to

$$\tilde{P}_{\Delta V} = \tilde{P}_{k|L} + \tilde{P}_{k+1|L}. \quad (25)$$

Real test cases will, of course, lie between these two extremes. Eq. (25) can also be used to produce a conservative estimate of the maneuver error covariance under any conditions. The following test cases will serve to explore the validity of the assumption that the cross covariance between the filter and smoother solutions is small.

TEST CASES

Two test cases are presented, one using a simulated reference trajectory and simulated measurements and one based on real measurements where a truth trajectory is not available. Both test cases were analyzed using STK/OD®, an orbit determination application built by Analytical Graphics, Inc.

Simulated Test Case

A test case was generated using simulated tracking data based on an orbit with the approximate parameters given in Table 1. An instantaneous in-track maneuver with nominal magnitude of 2 m/s is planned. The planned maneuver, the uncertainty associated with the planned maneuver and the actual simulated maneuver are given in Table 2. The maneuver is modeled based on its nominal values during the filtering and smoothing processes. The force model for the simulation consisted of Earth gravity (21x21), atmospheric drag (Jacchia 71), solar radiation pressure and third body perturbations. Process noise was added to the computation of atmospheric density and solar radiation pressure during the computation of the simulated trajectory. Measurements were simulated from the set of ground stations shown in Figure 1 and consisted of two-way range, two-way Doppler, azimuth and elevation at a frequency of one measurement set per minute. The measurements included time varying measurement biases and white noise.

TABLE 1. APPROXIMATE ORBIT PARAMETERS FOR SIMULATED TEST CASE

Epoch (GMT)	a (km)	e	I (deg)	Ω (deg)	ω (deg)	u (deg)
1 Jun 2002 12:00:00	6978.14	0.002	98.5	120.0	55.0	0.0

TABLE 2. SIMULATED MANEUVER

Epoch	2 Jun 2002 07:11:17.00 GMT		
	Nominal	Sigma	Simulated
Radial	0.0 m/s	0.035 m/s	0.0838 m/s
In-track	2.0 m/s	0.100 m/s	2.0701 m/s
Cross-track	0.0 m/s	0.035 m/s	-0.0513 m/s

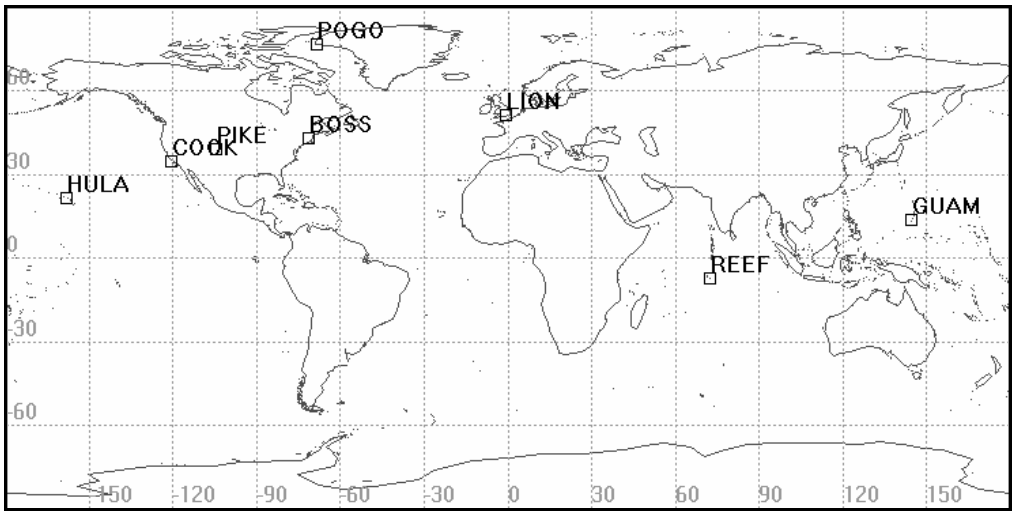

Figure 1. Tracking station locations

The simulation produced 30 passes of tracking data over a 19 hour interval before the maneuver and an additional 30 passes of tracking data in a 17 hour interval after the maneuver. The tracking data was simulated at a one minute step. The simulated maneuver time was between two tracking passes. The pass prior to the maneuver ended on 2 Jun 2002 06:16:30 and the first pass after the maneuver started at 07:43:00. Two covariance estimates were computed for the estimated maneuver. The proposed covariance was computed according to Eq. (20) and an additional covariance was computed according to Eq. (25). The second covariance estimate, which will be more conservative, was computed to determine the importance of the subtracted term in Eq. (20). The resulting maneuver estimate from the smoother is shown in Table 3. The covariance information in Table 3 is given in terms of the square roots of the variances of the proposed, σ, and the conservative, σ^*, estimates.

TABLE 3. ESTIMATED MANEUVER FROM SIMULATION

	Simulated (m/s)	Estimated (m/s)	Error (m/s)	σ (m/s)	σ^* (m/s)
Radial	0.0838	0.0805	-0.0033	0.006	0.025
In-track	2.0701	2.0696	-0.0005	0.002	0.006
Cross-track	-0.0513	-0.0460	0.0053	0.011	0.012

The results in Table 3 indicate that the smoothing process produced an accurate estimate of the simulated maneuver. The estimate of the maneuver uncertainty based on the application of Eq. (20) appears to be realistic while the estimate of the maneuver uncertainty based on Eq. (25) appears to be overly conservative. The realism of the covariance estimate will be examined further in the next section. An additional solution, given in Table 4, was computed where only one pass of tracking data was processed after the maneuver. The results indicate that the algorithm is able to produce a good result with a much smaller amount of post-maneuver tracking.

TABLE 4. ESTIMATED MANEUVER FROM SIMULATION (SINGLE PASS)

	Simulated (m/s)	Estimated (m/s)	Error (m/s)	σ (m/s)	σ^* (m/s)
Radial	0.0838	0.0667	-0.0171	0.018	0.043
In-track	2.0701	2.0739	0.0038	0.011	0.014
Cross-track	-0.0513	-0.0275	0.0238	0.030	0.031

Monte Carlo Analysis

A Monte-Carlo analysis was performed on the same simulation test case to validate the covariance associated with the maneuver estimate. Each run in the Monte-Carlo analysis consisted of selecting a new seed for the random number generator, then running the simulator followed by the filter and the smoother. This way a different set of random deviates was used in all elements of the truth trajectory, simulated maneuver and simulated measurements. The resulting maneuver estimate from the smoother was differenced with the simulated maneuver to produce the error in the maneuver estimate. This error, a three dimensional vector, was then rotated into the principle axis frame of the maneuver estimate error covariance. The principle axes and dimensions of the maneuver estimate covariance ellipsoid are found via a matrix decomposition of the form

$$\tilde{P}_{\Delta V(3x3)} = U^T D U \tag{26}$$

where $\tilde{P}_{\Delta V(3x3)}$, derived from the smoother, is the (3x3) sub-matrix containing the velocity components relevant to the maneuver, U is an orthogonal transformation matrix and D is a diagonal matrix. The elements of D are the variances in the principle axis frame and are therefore the squares of the dimensions of the one sigma ellipsoid. The matrix U provides the rotation from the reference axes of $\tilde{P}_{\Delta V(3x3)}$ to the principle axes of the ellipsoid.

A single measure of the error relative to the covariance is constructed by determining the n-sigma boundary on which the error lies. The value of n is found via the solution of the equation of the ellipsoid[4],

$$\left(U\, d\tilde{X}_{\Delta V}\right)^T \left(n^2 D\right)^{-1} \left(U\, d\tilde{X}_{\Delta V}\right) = 1, \tag{27}$$

where $d\tilde{X}_{\Delta V}$ is the error in the maneuver estimate and U serves to rotate the error into the principle axes frame. Eq. 27, which defines an ellipsoid with a surface of constant probability density for a Gaussian probability density function, is easily solved for n to give,

$$n = \sqrt{\frac{1}{\left(U\, d\tilde{X}_{\Delta V}\right)^T D^{-1} \left(U\, d\tilde{X}_{\Delta V}\right)}}. \tag{28}$$

The results of the Monte-Carlo analysis are plotted in a histogram and compared against the expected values for a three dimensional random vector in Figures 2-3. Figure 2 shows results based on the application of Eq. (20) while Figure 3 shows results based on the application of Eq. (25). The expected distribution is computed based upon the relationship between the probability level and the number of standard deviations, n, for a three dimensional random vector is given by[4],

$$prob_3(n) = erf\left(\frac{n}{\sqrt{2}}\right) - \sqrt{\frac{2}{p}} n\, e^{-\left(n^2/2\right)}. \tag{29}$$

The expected percentages (Gaussian 3D) in each bin of the histograms given in Figures 2 and 3 were computed as the difference in probabilities, for the values of n which bound the bin, multiplied by 100.

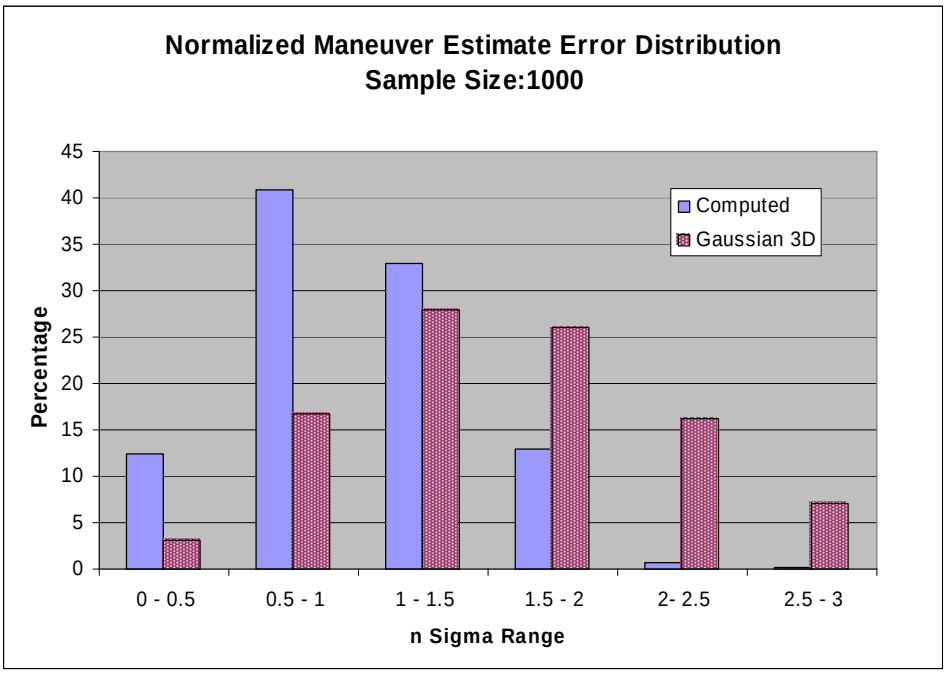

Figure 2. Normalized maneuver error distribution for proposed covariance

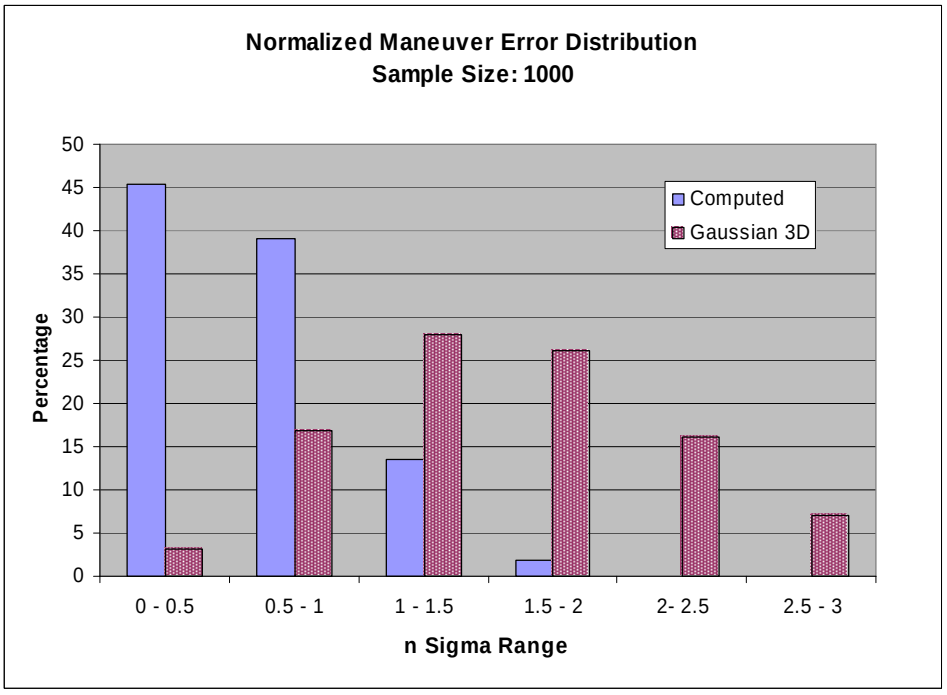

Figure 3. Normalized maneuver error distribution for conservative covariance

Figure 3 shows that the maneuver error covariance computed based on Eq. (25) is clearly too conservative. Figure 2 shows that the maneuver error covariance computed based on Eq. (20) is also conservative, but is better than the results of Figure 3. While the conservative appearance of the proposed result indicates that the assumption that the cross covariance between the filtered and smoothed estimates could be ignored may not be correct, a useful result is still obtained.

Real Data Test Case

Tracking data for the EO1 spacecraft was used for the real data test case. Approximate orbit elements for EO1 are given in Table 5. The tracking data consists of Doppler, azimuth and elevation from the single Data Lynx ground station, located in Alaska. Not all of the passes contained Doppler data. The overall span of tracking data started on 19 May 2002 and ended on 12 July 2002. The specific period of interest for this study was 13 Jun 2002 when two short duration maneuvers were performed. We did not have access to the nominal maneuver values, but we were given the duration of the maneuvers. The maneuvers were entered into the orbit determination software as having zero magnitude and spherical uncertainties based on the duration of the maneuvers. The summary of known and conjectured information on the maneuvers is given in Table 6.

TABLE 5. APPROXIMATE ORBIT PARAMETERS FOR EO1

Epoch (GMT)	a (km)	e	I (deg)	Ω (deg)	ω (deg)
19 May 2002	7085	0.0015	98.2	206.9	83.9

TABLE 6. MANEUVER INFORMATION

	Maneuver 1 at 14:08:00	Maneuver 2 at 16:35:44
Duration (sec)	45	26
Radial Sigma (cm/s)	20	10
In-track Sigma (cm/s)	20	10
Cross-track Sigma (cm/s)	20	10

The filter was run to process measurements across the time span of the maneuvers. The maneuvers were in the middle of a gap in the tracking data which started at 08:26:40 and lasted until 20:02:10 which means there is no tracking data between the maneuvers. Four passes of data after the maneuver were processed with the last pass ending at 14 Jun 2002 02:38:50. The smoothing process was then performed and the maneuver estimate from the

smoother is given in Table 7. We need to asses the validity of the smoothed estimates for the maneuvers. This was accomplished by inserting the smoothed estimates of the maneuvers into the filter and re-computing the Doppler residuals. Figures 4-5 show a comparison of the Doppler residuals for the first pass after the maneuvers for the cases where a zero maneuver was applied and the smoothed estimate of the maneuver was applied.

TABLE 7. SMOOTHED MANEUVER ESTIMATES

	Maneuver 1		Maneuver 2	
Epoch/Duration (sec)	14:08:00	45	16:35:44	26
Radial/Sigma (cm/s)	-2.7	7.3	-10.7	9.4
In-track/Sigma (cm/s)	11.2	1.0	-7.7	0.8
Cross-track/Sigma (cm/s)	3.2	11.2	-4.5	9.0

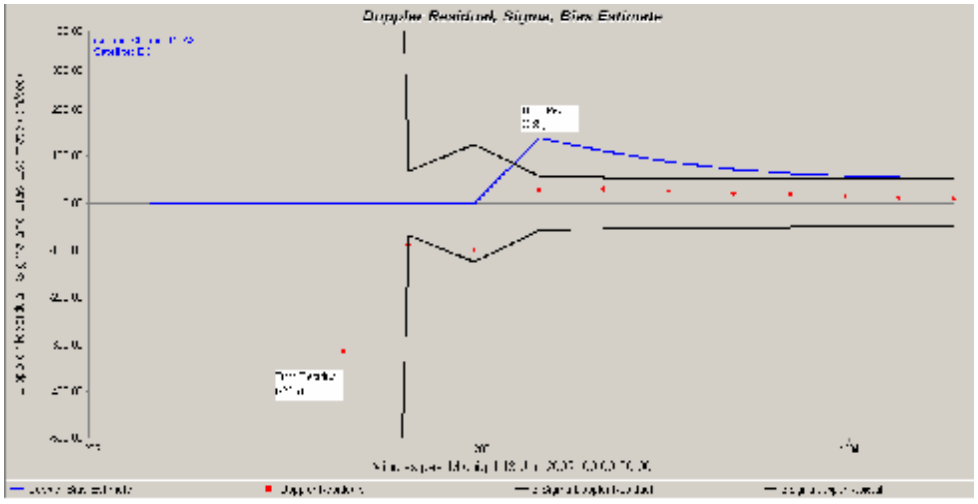

Figure 4. First pass Doppler residuals with zero maneuver

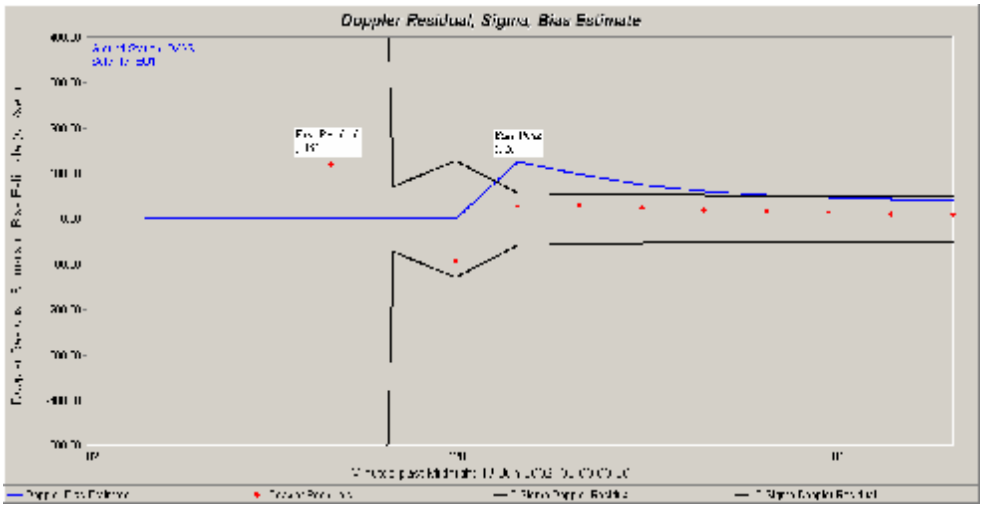

Figure 5. First pass Doppler residuals using first smoothed estimate

For the purpose of investigation, the process was iterated. A second smoother run, incorporating the maneuver estimate from the first smoother run, produced a second set of maneuver estimates. The same maneuver uncertainties were used in both runs. Comparisons of the first and second smoothed estimates for each of the maneuvers are given in Tables 8-9 while the effect of the second smoothed estimate on the Doppler residuals is shown in Figure 6. These comparisons indicate that performing the process twice yielded a minor improvement in the Doppler residuals and that the two estimates were consistent on the basis of their computed uncertainties.

TABLE 8. SMOOTHED MANEUVER 1 COMPARISON

	Estimate 1		Estimate 2	
Radial/Sigma (cm/s)	-2.7	7.3	-13.4	7.3
In-track/Sigma (cm/s)	11.2	1.0	10.7	1.0
Cross-track/Sigma (cm/s)	3.2	11.2	2.0	11.2

TABLE 9. SMOOTHED MANEUVER 2 COMPARISON

	Estimate 1		Estimate 2	
Radial/Sigma (cm/s)	-10.7	9.4	-17.3	9.4
In-track/Sigma (cm/s)	-7.7	0.8	-6.3	0.8
Cross-track/Sigma (cm/s)	-4.5	9.0	0.4	9.0

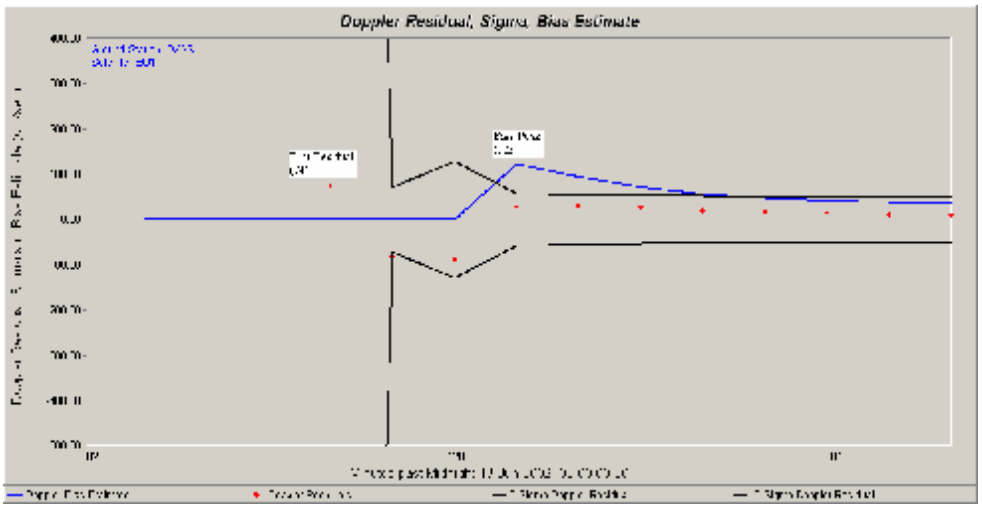

Figure 6. First pass Doppler residuals using second smoother estimate

CONCLUSIONS

A promising new method of solving for short duration maneuvers modeled as impulses in the orbit determination process has been developed. The process provides an estimate of the maneuver and an associated covariance with no additional work required by the operator. The amount of additional code required to perform the computations is extremely small and has virtually no effect on computational performance since the size of the estimation state is not altered. Simulations have been performed to verify the estimate and error covariance of the maneuver and a real data case has produced useful results. The resulting error covariance appears to be conservative, but is a substantial improvement over a covariance computed with the assumption that the pre-maneuver and post-maneuver estimates are not correlated. Additional Monte-Carlo analyses are required to fully characterize the performance of the algorithm.

ACKNOWLEGEMENTS

We would like to thank Dick Hujsak for his detailed review of this paper and many valuable comments.

REFERENCES

1. J. Carrico et al., "Maneuver Planning and Results for Clementine (The Deep Space Program Science Experiment)," Paper No. AAS 95-129, AAS/AIAA Spaceflight Mechanics Meeting, Albuquerque, New Mexico, February 1995.

2. Meditch, J. S., *Stochastic Optimal Linear Estimation and Control*. McGraw-Hill, New York, 1969.

3. Rauch, H. E., "Solutions to the Linear Smoothing Problem," *Transactions in Automated Control*, Vol. AC-8, 1963, p. 371.

4. Gura, I.A., Gersten, R.H., "On Analysis of n-Dimensional Normal Probabilities," Aerospace Report No. TR-0066(5129-01)-2.